Quasihydrostatic Equation of State of Iron above 2 Mbar

Agnès Dewaele,[1] Paul Loubeyre,[1] Florent Occelli,[1] Mohamed Mezouar,[2] Peter I. Dorogokupets,[3] and Marc Torrent[1]

[1]*DIF/Département de Physique Théorique et Appliquée, CEA, BP 12, 91680 Bruyères-le-Châtel, France*
[2]*European Synchrotron Radiation Facility, BP 220, F-38043 Grenoble Cedex, France*
[3]*Institute of the Earth's Crust SB RAS, Irkutsk 664033, Russia*

(Received 26 July 2006; published 22 November 2006)

The compression curve of iron is measured up to 205 GPa at 298 K, under quasihydrostatic conditions in a diamond anvil cell. Above 150 GPa, the compression of this metal is significantly higher than previously measured under nonhydrostatic conditions. The same compression curve is also calculated *ab initio* and the deviation between experiment and theory is clearly established. A formulation of the equation of state of iron over a large pressure and temperature range, based on the current data and existing shock-wave data, is also proposed. Implications for the Earth's core are discussed.

DOI: 10.1103/PhysRevLett.97.215504 PACS numbers: 62.50.+p, 07.35.+k, 64.30.+t

The equation of state (EOS) $P(V, T)$ is a fundamental characteristic of a material. With the advent of the diamond anvil cell, the most powerful static high pressure device, and the use of x-ray synchrotron diffraction, isothermal EOS of many elements have now been measured above 200 GPa [1]. Iron being the main component of the Earth's core, its EOS is also of major importance for our understanding of the physical state of this deep envelope. Several studies have thus been dedicated to the measurement of the EOS of ϵ-Fe (the hexagonal closed packed phase of iron, likely to be the thermodynamically stable phase of iron from 16 to at least 300 GPa [2]), either at ambient temperature up to 300 GPa [2] or at [300–1300 K] up to 300 GPa [3]. However, in these studies, no soft pressure transmitting medium has been used to compress iron above 80 GPa. The subsequent nonhydrostatic stresses on the sample can bias the x-ray diffraction measurements. For instance, systematic errors in volume and pressure measurements [4] or lattice distortions that can be misinterpreted as a phase transition [5,6] have been reported. It was recently shown that using helium as a pressure transmitting medium along with tiny samples, quasihydrostatic pressurizing conditions can be achieved in a diamond anvil cell above 100 GPa [7]. Using these data, the accuracy of calibration of pressure gauges for diamond anvil cells has been improved [7–10]. We decided to take advantage of these progresses and to investigate again the EOS of iron at ultrahigh pressure (up to 205 GPa) using similar techniques [7]. Our discussion will address three questions: is the new determination providing a significant difference over the previous determinations? Does the new data set allow determining if *ab initio* techniques are valid to calculate the properties of iron at high pressure? Does the new determination bring new insights for the properties of the Earth's core?

In five experimental runs (see Table I), an iron sample was embedded in a pressure transmitting medium and put a few micrometers away from the pressure gauge in the high pressure chamber of a diamond anvil cell. The high flux and high focusing of the x-ray beam of the ID27 beam line of ESRF [11] allowed collecting monochromatic x-ray diffracted signal in 1 min, even for the smallest samples (3 μm size). The pressure was measured from the luminescence of a ruby gauge or from the measurement of atomic volume of a tungsten x-ray gauge. This metal has been chosen because of its high x-ray scattering power and the accuracy of its EOS, attested by the consistency between static, dynamic, and ultrasonic measurements [7,8,12]. The calibrations of ruby and tungsten gauges have been taken from Ref. [8]. Uncertainty for this calibration can be estimated from the differences between published calibrations [7–10,12,13]: ± 1.5 at 100 GPa and ± 3 GPa at 200 GPa.

Our volume measurements are presented in Fig. 1 (see also supplementary materials [14]). Iron appears slightly stiffer, i.e., with larger volume, when compressed in neon (run 5) rather than in helium (runs 1–4). This suggests that the compression was less hydrostatic in run 5, which is confirmed by the larger scatter of x-ray reflections (see Table II). This could be explained by the lower quality of neon as a pressure transmitting medium, but also by a direct compression of the sample between the anvils in run 5 (the pressure chamber was extremely small, see Table I). Measured values of the c/a ratio for ϵ-Fe are reproducible, within a scatter of $\pm 1.2 \times 10^{-3}$. EOS parameters obtained by fitting the P-V data for compression in helium are presented in Table III, along with previously published values. It can be seen in Fig. 1 that from

TABLE I. Conditions of each experimental run. Sizes are in μm; PTM: pressure transmitting medium.

Run	P range (GPa)	P gauge	PTM	Diamond's culet size	Sample size	Symbol (Fig. 1)
1	0–34	ruby	He	400	10	+
2	18–47	ruby	He	400	10	−
3	36–124	ruby	He	100×300	4	×
4	28–197	tungsten	He	75×300	3	+
5	29–205	tungsten	Ne	50×300	3	*

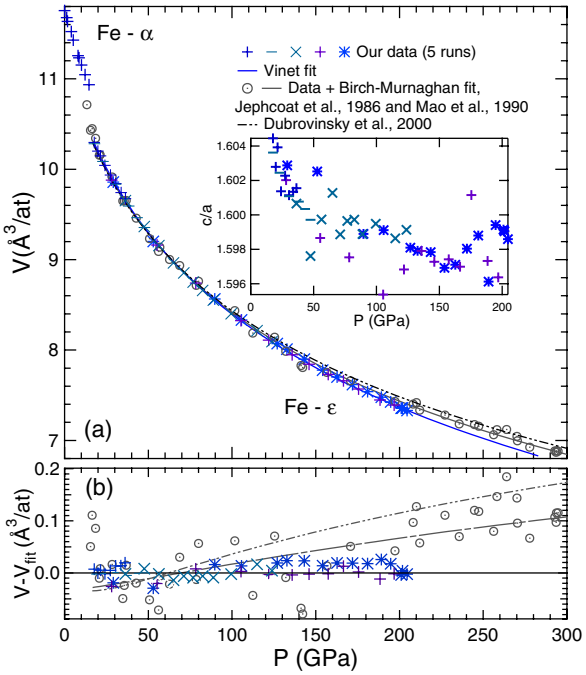

FIG. 1 (color online). (a) Measured atomic volume of iron (α-Fe for $P \leq 14.6$ GPa and ϵ-Fe for $P \geq 17.7$ GPa) as a function of the pressure (pressure gauge: see Table I), compared with literature data. Inset: evolution of the c/a ratio for hexagonal closed packed ϵ-Fe. (b) Difference between measured and fitted volume, Vinet formulation with $V_0 = 11.214$ Å^3, $K_0 = 163.4$ GPa, $K_0' = 5.38$.

$P \simeq 150$ GPa, the current compression curve significantly deviates from previous measurements [2,3]. Nonhydrostatic stresses in the previous experiments can qualitatively explain this discrepancy [4]. Moreover, the calibration of the platinum x-ray gauge used in Refs. [2,3] overestimates the pressure [7]. At 200 GPa, we measured a volume lower than in Refs. [2,3] by, respectively, 0.9% and 1.5%, a difference that doubles after extrapolation to 329 GPa (the pressure of the Earth's outer-inner core boundary). The corresponding compressibility increases are, respectively, 9.5% and 14% at 329 GPa.

We have also calculated the EOS of ϵ-Fe using one of the most advanced density-functional methods: the projected augmented wave (PAW) method [17,18] implemented in the ABINIT code [19]. This method can be considered as a combination of the pseudopotential approach with augmented wave methods that have been already used to *ab initio* predict the EOS of ϵ-Fe [20]. In the latter study, several possible magnetic orders of ϵ-Fe have been investigated and the lowest energy of the system has been obtained for an antiferromagnetic order (called afmII). However, magnetism has never been evidenced experimentally in ϵ-Fe. We thus calculated the EOS of both nonmagnetic (NM) and afmII ϵ-Fe. We treated $3s$, $3p$, $3d$, $4s$, $4p$ states as valence electrons. Local PAW basis with 2 projectors per angular momentum have been used and the generalized gradient approximation (GGA) exchange-correlation functional has been chosen [21]. The cutoff radius used for localized orbitals is 2.1 Bohr. The Brillouin zone sampling (respectively, 150 and 125 k points for NM and afmII ϵ-Fe) and the cutoff energy of the plane waves basis (10 Ry) have been adjusted to ensure that energies are converged to 0.1 mhartree/atom. The current calculations confirm (see Fig. 2) that the EOS of afmII ϵ-Fe is in better agreement with experimental data than EOS of NM ϵ-Fe at moderate pressures. Indeed, an equilibrium volume of 10.99 Å^3, only 2% lower than the experimental V_0, and a bulk modulus of 149 GPa are obtained by fitting the low pressure part of afmII ϵ-Fe EOS. This agreement has thus been improved by the use of PAW formalism. The magnetic moment vanishes around 50 GPa, and as a consequence, the EOS of NM and afmII phases become undistinguishable above that pressure. However, the subsequent kink in the EOS of afmII ϵ-iron (see Fig. 2) is not observed experimentally. This suggests a deficiency in the modeling of magnetic effects in ϵ-iron. Above $\simeq 100$ GPa, *ab initio* GGA EOS exhibits the usual pressure overestimation [7], by $\simeq 6\%$ at 300 GPa (or $\Delta V/V \simeq 1.3\%$). The accuracy of the prediction of ϵ-iron EOS by first principle methods has thus been brought within a $[-2\%, 1.3\%]$ range by this work.

We constructed a semiempirical high pressure and high temperature EOS of ϵ-Fe, based on the current ambient temperature data, Hugoniot data [22], and *ab initio* modeling [23]. At V and T, the total pressure can be

TABLE II. Examples of measured reflections for ϵ-iron in the two highest pressure runs. $\Delta d = d_{obs} - d_{calc}$, d_{obs} and d_{calc} being the interreticular distances, respectively, measured by individual peak fitting and calculated using the lattice parameters obtained by LeBail refinement of the whole spectrum (GSAS package [15]).

	Run 4, 197 GPa $a = 2.2030$ Å, $c = 3.5168$ Å		Run 5, 205 GPa $a = 2.1960$ Å, $c = 3.5105$ Å	
hkl	d_{obs} (Å)	$\Delta d/d_{obs}$	d_{obs} (Å)	$\Delta d/d_{obs}$
002	1.7581	-1.6×10^{-4}	1.7542	-5.7×10^{-4}
011	1.6771	8×10^{-5}	1.6727	3.2×10^{-4}
012	1.2929	-8×10^{-5}	1.2898	-3×10^{-5}
110	1.1015	$\simeq 0$	1.0986	5.7×10^{-4}
112	0.9334	-6×10^{-5}	0.9312	3.8×10^{-4}
021	0.9207	6×10^{-5}	0.9177	-1.2×10^{-4}

TABLE III. Parameters of the EOS obtained by least-squares fit of the experimental compression data for ϵ-Fe. The parameters of these EOS (Birch-Murnaghan, BM or Vinet, V, see Ref. [16] for a review of EOS formulations) are V_0, volume, K_0, bulk modulus, and K_0', its pressure derivative, under ambient conditions. Numbers between parenthesis are published error bars [2] or fitting error bars (95% confidence interval) on the last or the two last digits.

Reference	V_0 (Å^3)	K_0 (GPa), K_0'	P range (GPa)	Pressure medium	Pressure gauge	EOS
[2]	11.176(17)	165(4), 5.33(90)	35–300	Ar or none ($P \geq 80$ GPa)	Pt	BM
[3]	11.1989	156, 5.81	20–200	none (heating)	Pt	BM
This study	11.214(49)	163.4(7.9), 5.38(16)	17–197	He	ruby or W	V
This study	11.234(12)	165 (fixed), 4.97(4)	17–197	He	ruby or W	BM

expressed as [16]:

$$P(V,T) = P_V(V, 300\ \mathrm{K}) + (P_{\mathrm{TH}}(V,T) - P_{\mathrm{TH}}(V, 300\ \mathrm{K})). \quad (1)$$

We express $P_V(V, 300\ \mathrm{K})$ using our fitted Vinet EOS [16] (with parameters V_0, K_0, and K_0' from Table III, third row) and thermal pressure P_{TH} using a formalism simplified from Ref. [8]:

$$P_{\mathrm{TH}}(V,T) = \frac{9R\gamma}{V}\left(\frac{\theta}{8} + T\left(\frac{T}{\theta}\right)^3 \int_0^{\theta/T} \frac{z^3 dz}{e^z - 1}\right) + \frac{3R}{2V} m a_0 x^m T^2 + \frac{3R}{2V} g e_0 x^g T^2, \quad (2)$$

R being the gas constant and $x = V/V_0$. The first term of the right-hand side of Eq. (2) is the quasiharmonic Debye thermal pressure [16], which represents the main part of P_{TH}. The second and third terms are, respectively, the anharmonic and electronic thermal pressure. Their parameters a_0, m, e_0, and g have been obtained by fitting *ab initio* anharmonic and electronic thermal pressures [23] (the lack of accuracy of *ab initio* EOS is not expected to influence thermal pressures estimates, which are only weakly volume dependent): $a_0 = 3.7 \times 10^{-5}$ K^{-1}, $m = 1.87$, $e_0 = 1.95 \times 10^{-4}$ K^{-1}, $g = 1.339$.

In the Debye model, the Debye temperature θ varies only with volume: $d\ln\theta/d\ln V = -\gamma$, γ being the Grüneisen parameter. We chose the following form of γ: $\gamma = \gamma_\infty + (\gamma_0 - \gamma_\infty)x^\beta$, with $\beta = \gamma_0/(\gamma_0 - \gamma_\infty)$ (see Ref. [8]). We also fixed the Debye temperature of ϵ-iron under ambient conditions to 417 K [24]. Then the values of γ_0 and γ_∞ have been determined using shock-wave data up to 200 GPa (before any possible phase transition [25] and melting [26]), together with the current ambient temperature data, using a procedure described elsewhere [8]. The resulting values are $\gamma_0 = 1.875$ and $\gamma_\infty = 1.305$. We obtained a total thermal pressure in excellent agreement with the predictions of Ref. [23]. At 300 GPa and 6000 K, the values of quasiharmonic, anharmonic, and electronic terms are, respectively, 49, 3, and 15 GPa.

Iron is the major component of the Earth's core, alloyed with several percent of nickel and lighter elements (Si, O, S, etc. [27]). The EOS of this metal, under the relevant P-T conditions (136–329 GPa for the liquid outer core, 329–364 GPa for the solid inner core, and $T \simeq 5000$–6500 K), is compared to seismological measurements [28] to determine its chemical and physical state. Major geophysical issues thus rely directly on the accuracy of the EOS of

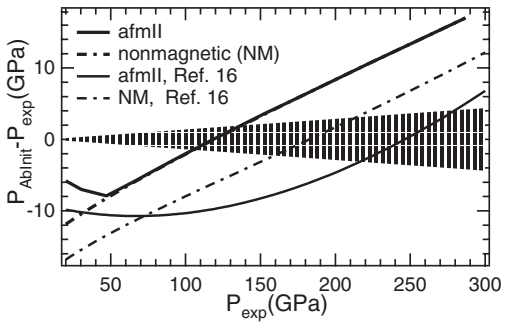

FIG. 2. Comparison between calculated DFT-GGA EOS (this work and Ref. [20]) and measured EOS. 298 K thermal pressure, calculated using Eq. (2), has been added to DFT-GGA pressure in order to be compared to P_{exp}. P_{Abinit}-P_{exp} is calculated for a given atomic volume V. The hatched area represents the uncertainty on P_{exp} caused by uncertainty on pressure calibration in the diamond anvil cell.

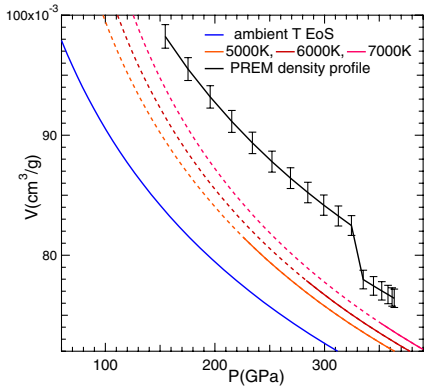

FIG. 3 (color online). Specific volume of ϵ-Fe as a function of pressure on several isotherms, calculated using Eqs. (1) and (2). The isotherms are plotted as continuous lines in the estimated domains of stability of solid iron [31]. Specific volume profile in the Earth's core, according to the PREM seismic model [28], is shown for comparison.

ϵ-iron. So far, even if a small density deficit of the inner core, compared to iron, had already been pointed out [2], it was not considered to be significant [3]. On this basis, light elements may be present in the outer core only.

The possible temperature in the inner core spans from $\simeq 5200$ K to $\simeq 6500$ K, from the estimated melting temperature of iron at the pressure of outer-inner core boundary [25,26]. Four isotherms (298, 5000, 6000, and 7000 K) calculated using Eqs. (1) and (2) are plotted in Fig. 3 together with a profile of specific volume in the Earth's core from the seismic preliminary reference Earth model (PREM) [28]. The Earth's inner core is lighter than ϵ-iron under the same conditions, which cannot be explained by the presence of nickel in the core because alloying of ϵ-iron with nickel is expected to increase, rather than decrease, its density (by approximately 0.4%, see Ref. [2]). We estimated this relative deficit at $\simeq$330 GPa: between 1.4% and 6.4% for $T = 6500$ K and 4.1% and 9.1% for $T = 5200$ K. These density differences take into account the uncertainties of PREM (1.5%) and of the current EOS. The bulk modulus K_S of ϵ-iron predicted by the current EOS is very close, within 1%, to the bulk modulus in the inner core [28].

The density deficit in the Earth's inner core can be interpreted in two different ways or a combination of the two. It can either be explained by the presence of light elements (like a molar fraction of (Si + S) of $10 \pm 7\%$) in this envelope. Chemical equilibrium calculations [29] and recent measurements of sound velocities [30] already led to a similar conclusion. Or, it could be a hint that the actual phase of iron in the inner core is not ϵ-Fe, but another solid phase with a lower density. The possibility of such a phase has already been inferred from a small discontinuity in shock-wave EOS above 200 GPa [25], and supported by theoretical calculations [31,32].

To sum up, the state-of-the-art conditions of our diamond anvil cell experiments, combined with x-ray diffraction, allowed us to improve the accuracy and reliability of ambient temperature EOS of ϵ-iron up to pressures relevant to the Earth's core. We also show that DFT, used with the most modern methods and approximations, can predict this EOS within 2% in volume, which is still less accurate than experiments. Experimental studies thus remain fundamental to explore the behavior of highly compressed matter. Using ambient temperature compression curve, we built a $P(V, T)$ EOS which suggests that the Earth's inner core is lighter than a mixture of ϵ-Fe and Ni under the same conditions.

The authors acknowledge the European Synchrotron Radiation Facility for provision of synchrotron radiation facilities on beam line ID27, during beam time allocated to proposal HS-2858. We thank C. Sanloup for her comments. Funding (P. I. D.) from RFBR (No. 05-05-64491) is gratefully acknowledged.

[1] E. Y. Tonkov and E. G. Ponyatovsky, *Phase Transformations of Elements under High Pressure* (CRC Press, Boca Raton, 2005).
[2] H.-K. Mao, Y. Wu, L. C. Chen, J. F. Shu, and A. P. Jephcoat, J. Geophys. Res. **95**, 21 737 (1990); A. P. Jephcoat, H.-K. Mao, and P. M. Bell, J. Geophys. Res. **91**, 4677 (1986).
[3] L. S. Dubrovinsky, S. K. Saxena, F. Tutti, S. Rekhi, and T. LeBehan, Phys. Rev. Lett. **84**, 1720 (2000).
[4] K. Takemura, J. Appl. Phys. **89**, 662 (2001).
[5] K. Takemura, Phys. Rev. Lett. **75**, 1807 (1995).
[6] K. Takemura, Phys. Rev. B **60**, 6171 (1999).
[7] A. Dewaele, P. Loubeyre, and M. Mezouar, Phys. Rev. B **70**, 094112 (2004).
[8] P. I. Dorogokupets and A. R. Oganov, Doklady Earth Sci. **410**, 1091 (2006); Phys. Rev. B (to be published).
[9] W. B. Holzapfel, High Press. Res. **25**, 187 (2005).
[10] A. D. Chijioke, W. J. Nellis, A. Soldatov, and I. F. Silvera, J. Appl. Phys. **98**, 114905 (2005).
[11] M. Mezouar *et al.*, J. Synchrotron Radiat. **12**, 659 (2005).
[12] W. Holzapfel, J. Appl. Phys. **93**, 1813 (2003).
[13] K. Kunc, I. Loa, and K. Syassen, Phys. Rev. B **68**, 094107 (2003).
[14] See EPAPS Document No. E-PRLTAO-97-048648 for raw *P-V* data. For more information on EPAPS, see http://www.aip.org/pubservs/epaps.html.
[15] R. von Dreele and A. C. Larson, Los Alamos National Laboratory Report No. LAUR 86-748, 1986 (unpublished).
[16] O. L. Anderson, *Equations of State of Solids for Geophysics and Ceramic Science* (Oxford University Press, New York, 1995).
[17] P. E. Blöchl, Phys. Rev. B **50**, 17 953 (1994).
[18] G. Kresse and D. Joubert, Phys. Rev. B **59**, 1758 (1999).
[19] X. Gonze *et al.*, Z. Kristallogr. **220**, 558 (2005).
[20] G. Steinle-Neumann, L. Stixrude, and R. E. Cohen, Phys. Rev. B **60**, 791 (1999).
[21] J. P. Perdew, K. Burke, and M. Ernzerhof, Phys. Rev. Lett. **77**, 3865 (1996).
[22] J. M. Brown, J. N. Fritz, and R. S. Hixson, J. Appl. Phys. **88**, 5496 (2000).
[23] D. Alfe, G. D. Price, and M. J. Gillan, Phys. Rev. B **64**, 045123 (2001).
[24] G. S. Shen *et al.*, Phys. Chem. Miner. **31**, 353 (2004).
[25] J. M. Brown, Geophys. Res. Lett. **28**, 4339 (2001).
[26] J. H. Nguyen and N. C. Holmes, Nature (London) **427**, 339 (2004).
[27] J.-P. Poirier, Phys. Earth Planet. Inter. **85**, 319 (1994).
[28] A. M. Dziewonski and D. L. Anderson, Phys. Earth Planet. Inter. **25**, 297 (1981).
[29] D. Alfè, M. J. Gillan, and G. D. Price, Nature (London) **405**, 172 (2000).
[30] J.-F. Lin, W. Sturhahn, J. Zhao, G. Shen, H.-K. Mao, and R. J. Hemley, Science **308**, 1892 (2005).
[31] A. B. Belonoshko, R. Ahuja, and B. Johansson, Nature (London) **424**, 1032 (2003).
[32] L. Vocadlo, D. Alfe, M. J. Gillan, I. G. Wood, J. P. Brodholt, and G. D. Price, Nature (London) **424**, 536 (2003).